may provide insight into the factors controlling multiple, proximal cleavage events on different strands.[31] Further experimentation will show whether this linearization is a result simply of the greater efficiency of cleavage by **3** or a special mechanism not available to **1** and **2**. In either event, it appears that complex **3** will provide a synthetic entry point into functionalized oxoruthenium(IV) cleavage agents with a wide range of DNA-binding properties and cleavage reactivity.

Conclusions

We have shown that cyclic voltammetry of **1**-**3** can be used to detect the noncovalent binding of the $Ru^{II}OH_2^{2+}$ forms to DNA and the cleavage of DNA by $Ru^{IV}O^{2+}$. The results show stronger binding of **2** by a factor of 5 relative to **1**, which binds more strongly than **3** by a factor of 3. This observation is consistent with studies on related complexes conducted using both electrochemical[2] and biochemical methods,[7] and we have observed stronger binding of **2** in a variety of biochemical experiments.[11] In the experiments described here, the stronger binding is evident in a larger decrease in current upon addition of the same amount of DNA to solutions that are the same concentration in metal complex. This decrease can be used to estimate the binding affinity. We have found that ITO working electrodes at 50 mM ionic strength allow for the accurate detection of binding in the absence of adsorption of the complex to the electrode; however, substantial adsorption of **2** to EOPG prohibits extraction of binding information using this electrode.

The electrocatalytic cleavage of DNA by $Ru^{IV}O^{2+}$ is apparent in a current enhancement in the IV/III couple. The detection of this catalytic current is complicated by the large contribution of current from quasi-reversible oxidation of free complex to the measured voltammogram, even in solutions where >90% of the complex is bound. Analysis of the difference in current for the IV/III and III/II couples upon addition of DNA (Figure 5) is a straightforward method for qualitatively assessing the degree of current enhancement. The efficiency of DNA cleavage upon controlled potential electrolysis is strongly influenced by the degree of binding of the complex to the DNA. Stronger binding of the complex in the $Ru^{II}OH_2^{2+}$ form leads to lower efficiency of electrocatalytic cleavage, because the active $Ru^{IV}O^{2+}$ form is generated at a slower rate.

Acknowledgment. We thank Professor E. F. Bowden for experimental assistance and helpful discussions. H.H.T. thanks the National Science Foundation for a Presidential Young Investigator Award (CHE-9157411), the David and Lucile Packard Foundation for a Fellowship in Science and Engineering, the Camille and Henry Dreyfus Foundation for a New Faculty Award, and the North Carolina Biotechnology Center for an Academic Research Initiation Grant. We also thank Professor F. M. Hawkridge for a gift of ITO.

Registry No. **1**, 20154-63-6; **2**, 101241-02-5; **3**, 127714-17-4; **3**$(ClO_4)_2$, 127714-24-3; Ru^{III}(tpy)(phen)$(OH)^{3+}$, 81971-63-3; Ru^{III}(tpy)(tmen)$(OH)^{3+}$, 140661-30-9; Ru^{IV}(tpy)(phen)O^{2+}, 98542-34-8; Ru^{IV}(tpy)(tmen)O^{2+}, 127714-19-6; Ru^{IV}(tpy)(bpy)O^{2+}, 73836-44-9.

Supplementary Material Available: Tables giving a summary of the crystal data and details of the X-ray data collection, atomic fractional coordinates, thermal parameters, and complete interatomic distances and angles and a drawing of **3**$(ClO_4)_2$ showing the complete atomic labeling (10 pages); a listing of observed and calculated structure factors (36 pages). Ordering information is given on any current masthead page.

(31) Basile, L. A.; Barton, J. K. *J. Am. Chem. Soc.* **1987**, *109*, 7548.

Contribution from the Department of Chemistry and Biochemistry, University of Colorado, Boulder, Colorado 80309

Semiquinone Imine Complexes of Ruthenium. Coordination and Oxidation of the 1-Hydroxy-2,4,6,8-tetra-*tert*-butylphenoxazinyl Radical

Samaresh Bhattacharya and Cortlandt G. Pierpont*

Received December 2, 1991

Reactions between $Ru(PPh_3)_3Cl_2$ and the 1-hydroxy-2,4,6,8-tetra-*tert*-butylphenoxazinyl radical (HPhenoxSQ) have been investigated. Stoichiometric reactions carried out under inert conditions with ratios of 1:1 and 1:2 for $Ru(PPh_3)_3Cl_2$ to HPhenoxSQ gave as products $Ru(PPh_3)_2Cl_2$(PhenoxSQ) and $Ru(PPh_3)Cl(PhenoxSQ)_2$, respectively. The complexes have been characterized spectrally, electrochemically, and structurally ($Ru(PPh_3)_2Cl_2$(PhenoxSQ), monoclinic, $P2_1/n$, a = 19.570 (6) Å, b = 14.652 (4) Å, c = 19.999 (7) Å, β = 91.65 (3)°, V = 5732 (3) Å^3, Z = 4, R = 0.032; $Ru(PPh_3)Cl(PhenoxSQ)_2$, monoclinic, $P2_1/c$, a = 10.228 (2) Å, b = 27.775 (8) Å, c = 23.656 (9) Å, β = 97.77 (2)°, V = 6658 (3) Å^3, Z = 4, R = 0.045). $Ru(PPh_3)_2Cl_2$(PhenoxSQ) is diamagnetic due to strong spin coupling between the radical and the $S = {}^1/_2$ metal ion; $Ru(PPh_3)Cl(PhenoxSQ)_2$ has a single unpaired electron. 2,4,6,8-Tetra-*tert*-butylphenoxazin-1-one (PhenoxBQ) has been characterized structurally (monoclinic, $P2_1/c$, a = 11.547 (4) Å, b = 17.659 (6) , c = 13.579 (3) Å, β - 105.92 (2)°, V = 2662 (1) Å^3, Z = 4, R = 0.063) to give metrical parameters for the benzoquinone imine ligand in its unreduced form. PhenoxBQ has also been characterized electrochemically. It undergoes two reversible reductions at potentials that are shifted negatively relative to related benzoquinone ligands. Increased energy of the PhenoxBQ π^* level relative to the energy of a benzoquinone antibonding electronic level results in an important difference in the order of energies of complex electronic levels. Reduction of $Ru(PPh_3)Cl(PhenoxSQ)_2$ occurs at the metal to give a Ru(II) product, while reduction of corresponding semiquinone complexes occurs at the quinone ligands. The electrochemical potential for reduction of $Ru(PPh_3)Cl(PhenoxSQ)_2$ is −1.02 V (Fc/Fc^+) and in its reduced form the complex is strongly nucleophilic. When the reaction between $Ru(PPh_3)_3Cl_2$ and HPhenoxSQ is carried out in air at a 1:2 stoichiometry, the product is a Ru(III) complex containing an oxidized form of PhenoxBQ. Two oxygen atoms and one hydroxyl group have been added to the coordinated PhenoxSQ ligand with ring-opening and cyclization leading to formation of a substituted dihydrofuran ring. The resulting complex $Ru(PPh_3)Cl$(PhenoxSQ)(OxPhenox) contains three chiral centers, two at carbon atoms and the third at the metal. Both oxygen addition and cyclization occur stereoselectively to give a single diastereomer. $Ru(PPh_3)Cl$(PhenoxSQ)(OxPhenox) has been characterized spectrally and structurally (monoclinic, $P2_1/c$, a = 19.092 (6) Å, b = 16.018 (7) Å, c = 24.889 (10) Å, β = 111.74 (3)°, V = 7070 (5) Å^3, Z = 4, R = 0.060). A mechanistic scheme is proposed for its formation by the reaction of reduced $Ru(PPh_3)Cl(PhenoxSQ)_2^-$, formed initially in the reaction, with molecular oxygen.

Introduction

Developments in the coordination chemistry of quinone ligands over the past 15 years have provided a number of surprising results. A general result that was unanticipated at the outset of this project is the exceptional stability and ubiquity of radical semiquinone complexes with transition-metal ions. The physical and chemical properties of these complexes have been a focus of interest. Magnetic spin coupling between a paramagnetic metal ion and the radical ligand is a specific physical property that has been found to occur characteristically for the semiquinone complexes.[1]

0020-1669/92/1331-2020$03.00/0

Table I. Crystallographic Data for PhenoxBQ, $Ru(PPh_3)_2Cl_2$(PhenoxSQ), $Ru(PPh_3)Cl$(PhenoxSQ)$_2$, and $Ru(PPh_3)Cl$(Phenox)(OxPhenox)

	PhenoxBQ	$Ru(PPh_3)_2Cl_2$(PhenoxSQ)	$Ru(PPh_3)Cl$(PhenoxSQ)$_2$	$Ru(PPh_3)Cl$(PhenoxSQ)(OxPhenox)
mol wt	421.6	1118.1	1242.0	1291.0
color	blue	green	brown	green
crystal system	monoclinic	monoclinic	monoclinic	monoclinic
space group	$P2_1/c$	$P2_1/n$	$P2_1/c$	$P2_1/c$
a, Å	11.547 (4)	19.570 (6)	10.228 (2)	19.092 (6)
b, Å	17.659 (6)	14.652 (4)	27.775 (8)	16.018 (7)
c, Å	13.579 (3)	19.999 (7)	23.656 (9)	24.889 (10)
β, deg	105.92 (2)	91.65 (3)	97.77 (2)	111.74 (3)
V, Å^3	2662 (1)	5732 (3)	6658 (3)	7070 (5)
Z	4	4	4	4
D_{calcd}, g cm^{-3}	1.052	1.296	1.239	1.213
D_{exptl}, g cm^{-3}	1.054	1.290	1.230	1.210
μ, mm^{-1}	0.060	0.458	0.341	0.326
T_{min}, T_{max}	0.791, 0.970	0.958, 0.967[b]	0.855, 0.986	0.923, 0.938[b]
R, R_w	0.063, 0.083	0.032, 0.042	0.045, 0.063	0.060, 0.067
GOF	2.11	1.35	1.44	1.21

[a] Radiation, Mo Kα (0.710 73 Å); temp, 294–297 K. [b] No correction applied.

Among the chemical reactions investigated with semiquinone and catecholate complexes, reactions with molecular oxygen have been of interest.[2] This is related to mechanistic features of enzymatic catechol oxidation[3] and to a commercial interest in the products that might be obtained from catechol oxidation processes.[4] The semiquinone ligands used in these studies contain oxygen donor atoms; far less work has been carried out with mixed nitrogen–oxygen donor benzoquinone imine ligands.[5] Mixed donor ligands are of interest, in part, because of their similarity to the quinoid-reduced pterins that appear to coordinate with iron or copper as cofactors in forms of phenylalanine hydroxylase.[6] More general interest is related to variation of parameters that influence the balance of charge between ligand and metal in the quinone complexes.[7] The increase in π orbital energy of the benzoquinone imines relative to simple benzoquinones would contribute to enhanced reactivity in complexes containing reduced forms of the quinone imine ligands, and complexes of this type that contain nucleophilic metals may be strongly reductive.

The subject of this report is the preparation and characterization of ruthenium complexes with the 1-hydroxy-2,4,6,8-tetra-*tert*-butylphenoxazinyl radical (HPhenoxSQ, I).[8] Studies on the

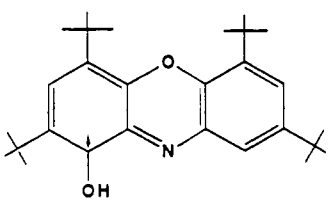

I

bis(semiquinone) complexes of ruthenium(III) have indicated that reduction occurs at the quinone ligands to give a mixed-charge Ru^{III}(SQ)(Cat) species.[9] This is a result of the balance of quinone and metal orbital energies, with the partially filled ligand π level below the vacant metal d-orbital. The vacant PhenoxSQ π level will likely be higher in energy than the vacant metal level resulting in reduction at the metal. Reduction of the Ru^{III}(PhenoxSQ)$_2$ unit would give a Ru^{II}(PhenoxSQ)$_2$ species with the metal ion existing as the reactive nucleophilic center. We describe herein the synthesis of PhenoxSQ complexes of ruthenium, their characterization by spectroscopic, structural, and electrochemical methods, and the reaction between a Ru^{II}(PhenoxSQ)$_2$ species with molecular oxygen that leads to a complex containing an oxidized form of the PhenoxBQ ligand.

Experimental Section

Materials. 2,4,6,8-Tetra-*tert*-butylphenoxazin-1-one (PhenoxBQ), 1-hydroxy-2,4,6,8-tetra-*tert*-butylphenoxazinyl radical (HPhenoxSQ), and $Ru(PPh_3)_3Cl_2$ were prepared according to literature procedures.[10,11]

Preparation of Complexes. $Ru(PPh_3)_2Cl_2$(PhenoxSQ). $Ru(PPh_3)_3Cl_2$ (200 mg, 0.21 mmol) and HPhenoxSQ (90 mg, 0.21 mmol) were combined and 40 mL of CH_2Cl_2 was distilled into the flask under N_2. The resulting blue-green solution was stirred for 30 min, and 40 mL of degassed hexane was layered over the solution. The volume of the solution was reduced with a slow flow of N_2 and dark green crystals of $Ru(PPh_3)_2Cl_2$(PhenoxSQ) separated from the solution. The crystals were collected by filtration and washed with hexane to give 175 mg of product in 75% yield.

$Ru(PPh_3)Cl$(PhenoxSQ)$_2$. $Ru(PPh_3)_3Cl_2$ (500 mg, 0.52 mmol) and HPhenoxSQ (490 mg, 1.16 mmol) were combined under Ar and 50 mL of degassed ethanol was added to the mixture of solids giving a dark brown solution. The solution was refluxed under argon for 2.5 h with stirring and the volume was reduced under a slow flow of Ar. The dark brown product was isolated by filtration, washed with dry degassed hexane, and recrystallized from a dichloromethane–hexane solution to give 500 mg of $Ru(PPh_3)Cl$(PhenoxSQ)$_2$ as dark brown crystals in 77% yield.

$Ru(PPh_3)Cl$(PhenoxSQ)(OxPhenox). $Ru(PPh_3)_3Cl_2$ (260 mg, 0.27 mmol) was added to a solution of HPhenoxSQ (280 mg, 0.66 mmol) in 50 mL of dried absolute ethanol. The mixture was refluxed in air for 4 h with stirring and then filtered. Solvent was removed from the filtrate under reduced pressure and the residue was throughly washed with hexane. The solid was recrystallized from a dichloromethane/hexane solution to give 220 mg of $Ru(PPh_3)Cl$(PhenoxSQ)(OxPhenox) as dark green crystals in 63% yield.

Physical Measurements. Electronic spectra were recorded on a Perkin-Elmer Lambda 9 spectrophotometer. Infrared spectra were obtained on an IBM IR/30 FTIR spectrometer with samples prepared as KBr pellets. ^{1}H NMR spectra were recorded on a Varian VXR 300S spectrometer. Cyclic voltammograms were obtained with a Cypress CYSY-1 computer-controlled electroanalysis system. A platinum disk working electrode and a platinum wire counter electrode were used. A Ag/Ag$^+$

(1) (a) Buchanan, R. M., Kessel, S. L.; Downs, H. H.; Pierpont, C. G.; Hendrickson, D. N. *J. Am. Chem. Soc.* **1978**, *100*, 7894. (b) Lynch, M. W.; Buchanan, R. M.; Pierpont, C. G.; Hendrickson, D. N. *Inorg. Chem.* **1981**, *20*, 1038.
(2) (a) Brown, D. G.; Beckmann, L.; Ashby, C. H.; Vogel, G. C.; Reinprecht, J. T. *Tetrahedron Lett.* **1977**, *1363*. (b) Speier, G. *J. Mol. Catal.* **1986**, *37*, 259.
(3) Cox, D. D.; Que, L., Jr. *J. Am. Chem. Soc.* **1988**, *110*, 8085.
(4) (a) Funabiki, T.; Tsujimoto, M.; Ozawa, S.; Yoshida, S. *Chem. Lett.* **1989**, 1267. (b) Demmin, T. R.; Swerdloff, M. D.; Rogic, M. M. *J. Am. Chem. Soc.* **1981**, *103*, 5795. (c) Oishi, N.; Nishida, Y.; Ida, K.; Kida, S. *Bull. Chem. Soc. Jpn.* **1980**, *53*, 2847. (d) Tatsuno, Y.; Nakamura, C.; Saito, T. *J. Mol. Catal.* **1987**, *42*, 57.
(5) (a) Masui, H.; Lever, A. B. P.; Auburn, P. R. *Inorg. Chem.* **1991**, *30*, 2402. (b) deLearie, L. A.; Haltiwanger, R. C.; Pierpont, C. G. *Inorg. Chem.* **1989**, *28*, 644. (c) Karsanov, I. V.; Ivakhnenko, Y. P.; Khandkarova, V. S.; Prokof'ev, A. I.; Rubezhov, A. Z.; Kabachnik, M. I. *J. Organomet. Chem* **1989**, *379*, 1.
(6) Dix, T. A.; Benkovic, S. J. *Acc. Chem. Res.* **1988**, *21*, 101.
(7) (a) Bhattacharya, S.; Pierpont, C. G. *Inorg. Chem.* **1992**, *31*, 35. (b) Bhattacharya, S.; Pierpont, C. G. *Inorg. Chem.* **1991**, *30*, 2906.
(8) Bhattacharya, S.; Boone, S. R.; Pierpont, C. G. *J. Am. Chem. Soc.* **1990**, *112*, 4561.
(9) (a) Lever, A. B. P.; Auburn, P. R.; Dodsworth, E. S.; Haga, M.; Liu, W.; Melnik, M.; Nevin, W. A. *J. Am. Chem. Soc.* **1988**, *110*, 8076. (b) Bhattacharya, S.; Pierpont, C. G. *Inorg. Chem.* **1991**, *30*, 1511.
(10) Stegmann, H. B.; Scheffler, K. *Chem. Ber.* **1968**, *101*, 262.
(11) Stephenson, T. A.; Wilkinson, G. *J. Inorg. Nucl. Chem.* **1966**, *28*, 945.

Table II. Selected Atomic Coordinates (×10⁴) for PhenoxBQ

	x/a	y/b	z/c
O1	3406 (4)	2861 (3)	228 (3)
O2	6478 (3)	1073 (2)	268 (2)
N1	5236 (3)	2015 (2)	1286 (3)
C1	4901 (4)	1959 (2)	289 (3)
C2	3871 (4)	2423 (3)	−265 (4)
C3	3448 (4)	2381 (3)	−1356 (3)
C4	4058 (4)	1897 (3)	−1805 (3)
C5	5073 (4)	1411 (2)	−1312 (3)
C6	5486 (4)	1471 (2)	−278 (3)
C7	6213 (4)	1597 (2)	1818 (3)
C8	6861 (4)	1135 (2)	1327 (3)
C9	7861 (4)	729 (2)	1891 (3)
C10	8133 (4)	808 (3)	2949 (3)
C11	7504 (4)	1249 (3)	3477 (3)
C12	6524 (4)	1651 (3)	2894 (3)
C13	2410 (5)	2865 (3)	−1952 (4)
C17	5575 (4)	865 (3)	−1963 (3)
C21	8661 (4)	248 (3)	1399 (4)
C25	7878 (5)	1277 (3)	4649 (3)

reference electrode was used that consisted of a CH_3CN solution of $AgPF_6$ in contact with a silver wire placed in glass tubing with a Vycor frit at one end to allow ion transport. Tetrabutylammonium hexafluorophosphate (TBHP) was used as the supporting electrolyte, and the ferrocene/ferrocenium couple was used as an internal standard. With this experimental arrangement the Fc/Fc^+ couple appeared at 0.159 V (vs Ag/Ag^+) with ΔE of 106 mV.

Crystallographic Structure Determination on 2,4,6,8-Tetra-*tert*-butylphenoxazin-1-one (PhenoxBQ). Dark blue crystals of PhenoxBQ were obtained as prismatic blocks from an acetone/ethanol solution. Axial photographs indicated monoclinic symmetry and the centered settings of 25 reflections in the 2θ range between 33° and 41° gave the unit cell dimensions listed in Table I. Data were collected by θ–2θ scans on a Seimens P3 diffractometer within the angular range 3.0° to 45.0°. Locations of the ring atoms and many of the *tert*-butyl atoms were determined by direct methods. Methyl carbon atoms of all four *tert*-butyl groups were found to be rotationally disordered and were refined with carbon atoms of fractional occupancy at disordered sites. Final cycles of least-squares refinement converged with discrepancy indices of R = 0.063 and R_W = 0.083. Final positional parameters for selected atoms of the PhenoxBQ molecule are listed in Table II. Tables containing a full listing of atom positions, anisotropic displacement parameters, and hydrogen atom locations are available as supplementary material.

Crystallographic Structure Determination on $Ru(PPh_3)_2Cl_2$(PhenoxSQ). Dark green crystals of $Ru(PPh_3)_2Cl_2$(PhenoxSQ) were obtained as thin plates from a hexane/dichloromethane solution. Axial photographs indicated monoclinic symmetry and the centered settings of 25 reflections in the 2θ range between 25° and 34° gave the unit cell dimensions listed in Table I. Data were collected by θ–2θ scans within the angular range 3.0° to 45.0°. The location of the metal atom was determined from a sharpened Patterson map. Phases based on a structure factor calculation containing the ruthenium were used to obtain the locations of other atoms of the structure. Final cycles of least-squares refinement converged with discrepancy indices of R = 0.032 and R_w = 0.042. Final positional parameters for selected atoms of the $Ru(PPh_3)_2Cl_2$(PhenoxSQ) molecule are listed in Table III. Tables containing a full listing of atom positions, anisotropic displacement parameters, and hydrogen atom locations are available as supplementary material.

Crystallographic Structure Determination on $Ru(PPh_3)Cl$(PhenoxSQ)$_2$. Dark brown crystals of $Ru(PPh_3)Cl(PhenoxSQ)_2$ were obtained as hexagonal paralelepipeds from a hexane/dichloromethane solution. Axial photographs indicated monoclinic symmetry and the centered settings of 25 reflections in the 2θ range between 18° and 35° gave the unit cell dimensions listed in Table I. Data were collected by θ–2θ scans within the angular range 3.0° to 45.0°. The location of the metal atom was determined from a sharpened Patterson map. Phases based on a structure factor calculation containing the ruthenium were used to obtain the locations of other atoms of the structure. Methyl carbon atoms of one *tert*-butyl group were rotationally disordered and were refined with two sets of carbon atoms of fractional occupancy. Final cycles of least-squares refinement converged with discrepancy indices of R = 0.045 and R_w = 0.053. Final positional parameters for selected atoms of the $Ru(PPh_3)Cl(PhenoxSQ)_2$ molecule are listed in Table IV. Tables containing a full listing of atom positions, anisotropic displacement parameters, and hydrogen atom locations are available as supplementary material.

Table III. Selected Atomic Coordinates (×10⁴) for $Ru(PPh_3)_2Cl_2$(PhenoxSQ)

	x/a	y/b	z/c
Ru	2563 (1)	2343 (1)	911 (1)
Cl1	3019 (1)	2192 (1)	2032 (1)
Cl2	2875 (1)	757 (1)	765 (1)
O1	2372 (1)	3689 (2)	1059 (1)
O2	1700 (1)	3520 (2)	−1222 (1)
N	2153 (2)	2714 (2)	8 (1)
C1	2053 (2)	3629 (2)	−65 (2)
C2	2175 (2)	4156 (2)	535 (2)
C3	2057 (2)	5112 (2)	517 (2)
C4	1891 (3)	5465 (3)	−101 (2)
C5	1786 (2)	4993 (2)	−716 (2)
C6	1841 (2)	4061 (2)	−670 (2)
C7	1936 (2)	2182 (2)	−550 (2)
C8	1702 (2)	2586 (2)	−1149 (2)
C9	1457 (2)	2053 (2)	−1687 (2)
C10	1488 (2)	1118 (3)	−1603 (2)
C11	1719 (2)	682 (2)	−1025 (2)
C12	1929 (2)	1238 (2)	−496 (2)
C13	2099 (3)	5726 (3)	1142 (2)
C17	1669 (3)	5523 (3)	−1369 (2)
C21	1119 (2)	2471 (3)	−2323 (2)
C25	1745 (2)	−356 (3)	−947 (2)
P1	3723 (1)	2533 (1)	538 (1)
P2	1455 (1)	1991 (1)	1357 (1)

Table IV. Selected Atomic Coordinates (×10⁴) for $Ru(PPh_3)Cl(PhenoxSQ)_2$

	x/a	y/b	z/c
Ru	2182 (1)	1030 (1)	3047 (1)
O1	3625 (4)	1250 (2)	3671 (2)
O2	2739 (4)	2688 (1)	2615 (2)
O3	939 (4)	1412 (1)	3463 (2)
O4	−1818 (4)	1118 (1)	1737 (2)
N1	2652 (4)	1687 (2)	2734 (2)
N2	527 (4)	963 (2)	2486 (2)
P	1651 (2)	333 (1)	3560 (1)
Cl	3801 (2)	693 (1)	2518 (1)
C1	3266 (6)	1971 (2)	3157 (3)
C2	3787 (6)	1719 (2)	3666 (3)
C3	4455 (6)	1988 (2)	4120 (3)
C4	4562 (6)	2476 (2)	4032 (3)
C5	4058 (6)	2736 (2)	3539 (3)
C6	3387 (6)	2472 (2)	3102 (3)
C7	2317 (5)	1898 (2)	2202 (2)
C8	2278 (6)	2399 (2)	2153 (3)
C9	1733 (6)	2615 (2)	1640 (3)
C10	1480 (6)	2310 (2)	1174 (3)
C11	1673 (6)	1814 (2)	1190 (3)
C12	2030 (5)	1604 (2)	1720 (3)
C13	4926 (8)	1762 (3)	4690 (3)
C17	4256 (7)	3289 (2)	3511 (3)
C21	1383 (7)	3153 (2)	1587 (3)
C25	1484 (7)	1520 (2)	640 (3)
C29	−339 (5)	1321 (2)	2576 (3)
C30	−59 (6)	1574 (2)	3101 (3)
C31	−889 (6)	1952 (2)	3221 (3)
C32	−1909 (6)	2062 (2)	2799 (3)
C33	−2254 (6)	1818 (2)	2278 (3)
C34	−1490 (6)	1422 (2)	2197 (3)
C35	107 (5)	636 (2)	2053 (2)
C36	−1090 (6)	703 (2)	1700 (3)
C37	−1574 (6)	352 (2)	1296 (3)
C38	−736 (6)	−33 (2)	1236 (3)
C39	487 (6)	−98 (2)	1558 (3)
C40	899 (6)	240 (2)	1972 (3)
C41	−649 (6)	2238 (3)	3778 (3)
C45	−3357 (6)	2006 (3)	1832 (3)
C49	−2963 (7)	372 (3)	949 (3)
C53	1381 (7)	−530 (3)	1464 (3)

Crystallographic Structure Determination on $Ru(PPh_3)Cl$(PhenoxSQ)(OxPhenox). Dark green crystals of $Ru(PPh_3)Cl$(PhenoxSQ)(OxPhenox) were obtained as hexagonal parallelepipeds from a hexane/dichloromethane solution. Axial photographs indicated monoclinic symmetry and the centered settings of 25 reflections in the 2θ range

Table V. Selected Atomic Coordinates ($\times 10^4$) for $Ru(PPh_3)Cl(PhenoxSQ)(OxPhenox)$

	x/a	*y/b*	*z/c*
Ru	1373 (1)	4917 (1)	1870 (1)
Cl	1473 (2)	3424 (2)	1818 (2)
P	1203 (2)	6375 (2)	1682 (3)
O1	219 (4)	4844 (5)	1539 (3)
O2	649 (4)	5048 (6)	3511 (3)
O3	1467 (4)	4885 (6)	1084 (3)
O4	4063 (5)	4570 (5)	2275 (4)
O5	3696 (5)	5462 (6)	1474 (4)
O6	2220 (5)	4368 (6)	660 (4)
O7	3150 (7)	5590 (7)	458 (5)
N1	1124 (6)	4834 (6)	2583 (4)
N2	2566 (5)	4969 (7)	2078 (3)
C1	394 (7)	4936 (8)	2498 (4)
C2	−112 (6)	4921 (8)	1904 (5)
C3	−891 (6)	4954 (9)	1773 (5)
C4	−1115 (7)	5097 (9)	2231 (5)
C5	−637 (7)	5206 (8)	2829 (5)
C6	98 (7)	5061 (8)	2948 (5)
C7	1563 (7)	4529 (7)	3143 (5)
C8	1324 (7)	4651 (7)	3603 (5)
C9	1735 (7)	4351 (7)	4162 (5)
C10	2363 (7)	3871 (8)	4210 (6)
C11	2604 (8)	3675 (8)	3755 (6)
C12	2211 (7)	4067 (8)	3229 (5)
C13	−1470 (8)	4825 (11)	1153 (6)
C17	−1002 (8)	5402 (9)	3262 (6)
C21	1534 (8)	4515 (10)	4679 (7)
C25	3268 (8)	3088 (8)	3854 (6)
C29	2738 (7)	4702 (7)	1654 (5)
C30	3566 (7)	4678 (8)	1683 (6)
C31	3765 (8)	4027 (9)	1320 (6)
C32	3953 (9)	4415 (10)	939 (7)
C33	3813 (11)	5339 (10)	932 (8)
C34	2098 (8)	4618 (8)	1085 (5)
C35	3167 (7)	5199 (7)	2605 (5)
C36	3899 (6)	5001 (9)	2689 (4)
C37	4499 (8)	5163 (8)	3215 (6)
C38	4290 (8)	5645 (8)	3601 (6)
C39	3572 (8)	5914 (8)	3532 (5)
C40	3000 (7)	5668 (7)	3027 (5)
C41	3758 (8)	3083 (9)	1407 (7)
C45	4418 (14)	5890 (12)	904 (9)
C49	5297 (7)	4864 (10)	3341 (6)
C53	3456 (9)	6421 (9)	4012 (6)

between 16° and 24° gave the unit cell dimensions listed in Table I. Data were collected by θ–2θ scans within the angular range 3.0° to 45.0°. The location of the metal atom was determined from a sharpened Patterson map. Phases based on a structure factor calculation containing the ruthenium were used to obtain the locations of other atoms of the structure. Final cycles of least-squares refinement converged with discrepancy indices of $R = 0.060$ and $R_w = 0.067$. Final positional parameters for selected atoms of the $Ru(PPh_3)Cl(PhenoxSQ)(OxPhenox)$ molecule are listed in Table V. Tables containing a full listing of atom positions, anisotropic displacement parameters, and hydrogen atom locations were deposited with our earlier communication on this structure determination.[8]

Experimental Results

Few studies have been carried out on *o*-benzoquinone imine complexes that take advantage of the redox activity of the ligand.[5] The PhenoxBQ ligand can be obtained by the reaction between 3,5-di-*tert*-butylcatechol and aqueous ammonium hydroxide when carried out in air.[10] The *tert*-butyl substituents of the catechol have proven to be quite helpful in the characterization of complexes formed with DBCat, and this feature appears to be carried over to the Phenox complexes. The imine nitrogen of PhenoxBQ would be expected to be a stronger donor than the oxygen atoms of the unreduced benzoquinone and would facilitate coordination of the unreduced form of PhenoxBQ. Reduction of the iminoquinone would be expected to occur at more negative potentials than corresponding benzoquinones. Structural and electrochemical characterizations on uncoordinated PhenoxBQ have been carried out as a preliminary step in the investigation of its coordination properties.

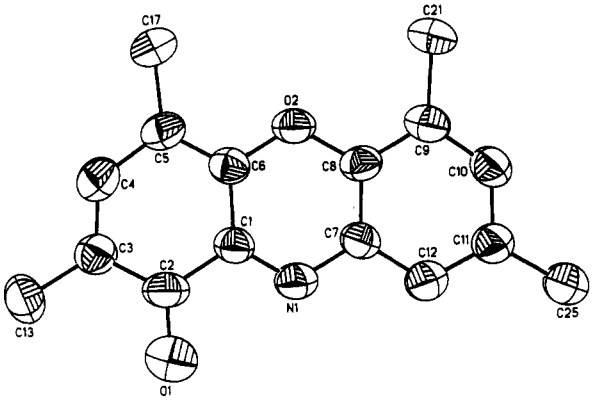

Figure 1. View of the PhenoxBQ molecule. Methyl carbon atoms of the *tert*-butyl groups have been omitted.

Table VI. Selected Bond Lengths and Angles for PhenoxBQ

	Lengths (Å)		
O1–C2	1.239 (7)	O2–C6	1.375 (5)
O2–C8	1.388 (5)	N1–C1	1.305 (6)
N1–C7	1.375 (5)	C1–C2	1.470 (6)
C1–C6	1.441 (7)	C2–C3	1.429 (6)
C3–C4	1.356 (7)	C3–C13	1.514 (7)
C4–C5	1.458 (6)	C5–C6	1.357 (6)
C5–C17	1.526 (7)	C7–C8	1.394 (7)
C7–C12	1.410 (6)	C8–C9	1.396 (6)
C9–C10	1.390 (7)	C9–C21	1.537 (7)
C10–C11	1.391 (7)	C11–C12	1.385 (6)
C11–C25	1.531 (6)		
	Angles (deg)		
C6–O2–C8	120.0 (3)	C1–N1–C7	118.1 (4)
N1–C1–C2	117.2 (4)	N1–C1–C6	123.4 (4)
C2–C1–C6	119.5 (4)	O1–C2–C1	118.8 (4)
O1–C2–C3	121.1 (4)	C1–C2–C3	120.0 (4)
C2–C3–C4	115.3 (4)	C2–C3–C13	121.4 (4)
C4–C3–C13	123.3 (4)	C3–C4–C5	128.0 (4)
C4–C5–C6	116.1 (4)	C4–C5–C17	119.4 (4)
C6–C5–C17	124.5 (4)	O2–C6–C1	117.5 (3)
O2–C6–C5	121.5 (4)	C1–C6–C5	121.1 (4)
N1–C7–C8	122.2 (4)	N1–C7–C12	116.6 (4)
C8–C7–C12	121.2 (4)	O2–C8–C7	118.8 (3)
O2–C8–C9	120.6 (4)	C7–C8–C9	120.7 (4)
C8–C9–C10	115.7 (4)	C8–C9–C21	123.4 (4)
C10–C9–C21	120.8 (4)	C9–C10–C11	126.0 (4)
C10–C11–C12	116.9 (4)	C10–C11–C25	121.1 (4)
C12–C11–C25	122.0 (5)	C7–C12–C11	119.6 (4)

2,4,6,8-Tetra-*tert*-butylphenoxazin-1-one (PhenoxBQ). A view showing the PhenoxBQ molecule is given in Figure 1 and selected bond distances and angles are contained in Table VI. The carbonyl C2–O1 bond length is 1.239 (7) Å, typical of a double C–O bond length, and the C1–N1 length is 1.305 (6) Å, typical of a localized C–N double bond. Bond lengths about the quinone ring show the pattern expected of a localized benzoquinone with short values for C3–C4 and C5–C6 (1.357 (7) Å) and longer values for the other C–C lengths of the ring. Bond lengths to oxygen O2 are typical of single C–O bonds, the N1–C7 length is 1.375 (5) Å, also a single bond length, and ring C–C lengths of the outer ring containing C7 to C12 are typical of delocalized aromatic values. The tricyclic core of the molecule is essentially planar with a dihedral angle between rings at the N, O bridge of 2.4°.

Structural features of the PhenoxBQ molecule show that the iminoquinone region of the molecule is electronically isolated from the aromatic ring with no structural indications of conjugation across the nitrogen or oxygen atoms connecting the two rings.

Cyclic voltammograms on PhenoxBQ shown in Figure 2 and listed in Table VII consist of two one-electron reduction steps. The first is reversible and appears at a potential of −1.249 V (vs Fc/Fc^+); the second is irreversible and appears at −2.147 V. Reduction of PhenoxBQ to give PhenoxSQ occurs at a potential which is 200 mV more negative than the DBBQ/DBSQ reduction

Table VII. Electrochemical Data for PhenoxBQ, $Ru(PPh_3)_2Cl_2$(PhenoxSQ), $Ru(PPh_3)Cl(PhenoxSQ)_2$, and $Ru(PPh_3)Cl$(Phenox)(OxPhenox)

compound	$E_{1/2}$, V vs Fc/Fc^+ (ΔE, mV)[a]			
	OxII	OxI	RedI	RedII
PhenoxBQ			−1.249 (98)	−2.147 (E_{pc})
$Ru(PPh_3)_2Cl_2$(PhenoxSQ)	0.584 (E_{pa})	0.287 (86)	−1.119 (E_{pc})	
$Ru(PPh_3)Cl(PhenoxSQ)_2$	0.875 (92)	−0.254 (102)	−1.026 (94)	
$Ru(PPh_3)Cl$(PhenoxSQ)(OxPhenox)		0.564 (75)	−0.933 (82)	

[a] In dichloromethane (0.1 M TBAP) at 23 °C. $E_{1/2}$ = half-wave potential, ΔE = peak separation between anodic and cathodic peaks of CV.

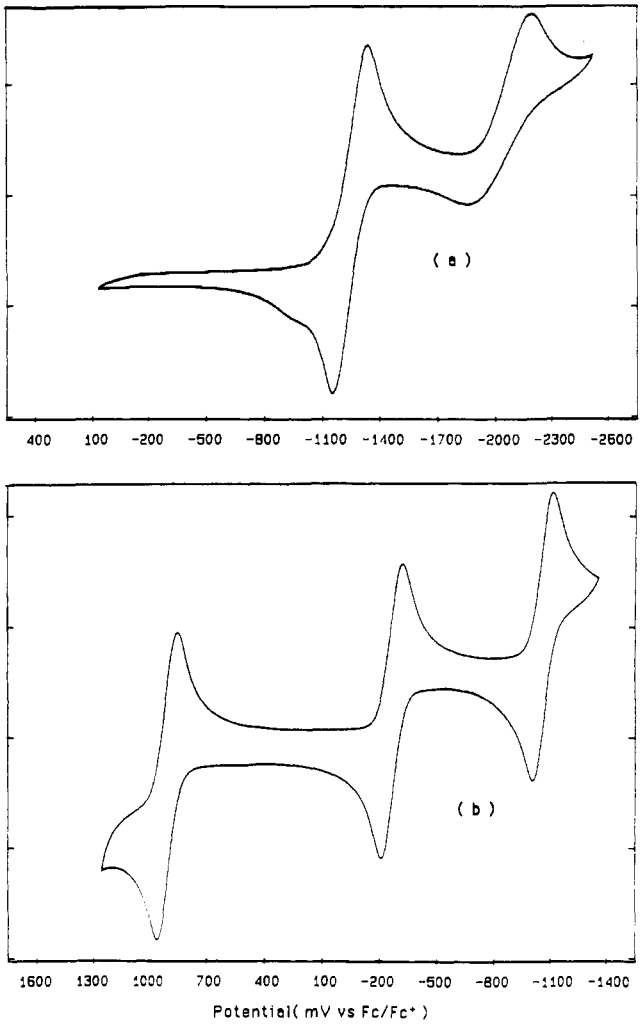

Figure 2. Cyclic voltammograms showing (a) the reductions of PhenoxBQ and (b) the reduction and oxidations of $Ru(PPh_3)Cl(PhenoxSQ)_2$. Dichloromethane was used as the solvent; scan rates were 100 mV/s.

potential of 3,5-di-*tert*-butyl-1,2-benzoquinone (DBBQ), and the second reduction step is nearly 0.5 V more negative than the corresponding reduction to DBCat.

$Ru(PPh_3)_2Cl_2$(PhenoxSQ). The product obtained from the reaction between $Ru(PPh_3)_3Cl_2$ and HPhenoxSQ carried out at a stoichiometric ratio of 1:1 is $Ru(PPh_3)_2Cl_2$(Phenox). Two charge distributions are possible for the complex, either Ru(II)–PhenoxBQ or Ru(III)–PhenoxSQ. The complex is diamagnetic and shows four sharp *tert*-butyl resonances in its ^1H NMR spectrum at 1.11, 1.29, 1.45, and 1.50 ppm. Electronic spectra recorded in dichloromethane consist of bands in the visible region at 410 nm (6400 M^{-1} cm^{-1}), with a shoulder at 480 nm, and 633 nm (8000), with a shoulder at 760 nm. A view of the complex molecule is shown in Figure 3, and bond distances and angles are listed in Table VIII. Phosphine ligands are coordinated at trans sites about the metal with phenyl rings of each ligand stacked above and below the plane of the Phenox lignad. Features of the Phenox ligand provide information on charge in the same way that features of quinone ligands allow differentiation between benzoquinone, semiquinone, and catecholate electronic forms. The quinone

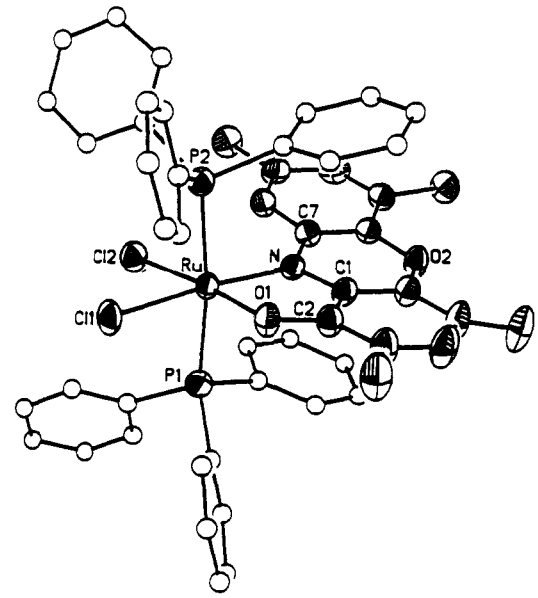

Figure 3. View of $Ru(PPh_3)_2Cl_2$(PhenoxSQ).

Table VIII. Selected Bond Lengths and Angles for $Ru(PPh_3)_2Cl_2$(PhenoxSQ)

Lengths (Å)			
Ru–Cl1	2.400 (1)	Ru–Cl2	2.422 (1)
Ru–O1	2.030 (2)	Ru–N	2.029 (3)
Ru–P1	2.427 (1)	Ru–P2	2.424 (1)
O1–C2	1.300 (4)	O2–C6	1.380 (4)
O2–C8	1.377 (4)	N–C1	1.363 (4)
N–C7	1.417 (4)	C1–C2	1.442 (5)
C1–C6	1.417 (5)	C2–C3	1.420 (5)
C3–C4	1.370 (6)	C3–C13	1.541 (6)
C4–C5	1.421 (5)	C5–C6	1.372 (5)
C5–C17	1.530 (6)	C7–C8	1.401 (5)
C7–C12	1.388 (5)	C8–C9	1.402 (5)
C9–C10	1.382 (5)	C9–C21	1.544 (5)
C10–C11	1.385 (5)	C11–C123	1.388 (5)
C11–C25	1.529 (5)		
Angles (deg)			
Cl1–Ru–Cl2	86.4 (1)	Cl1–Ru–O1	91.1 (1)
Cl2–Ru–O1	175.8 (1)	Cl1–Ru–N	169.5 (1)
Cl2–Ru–N	104.1 (1)	O1–Ru–N	78.5 (1)
Cl1–Ru–P1	88.4 (1)	Cl2–Ru–P1	80.3 (1)
O1–Ru–P1	96.3 (1)	N–Ru–P1	92.5 (1)
Cl1–Ru–P2	87.1 (1)	Cl2–Ru–P2	94.1 (1)
O1–Ru–P2	89.0 (1)	N–Ru–P2	92.8 (1)
P1–Ru–P2	173.1 (1)	Ru–O1–C2	116.5 (2)
C6–O2–C8	119.1 (2)	Ru–N–C1	114.3 (2)
Ru–N–C7	131.0 (2)	C1–N–C7	114.7 (3)
N–C1–C2	114.7 (3)	N–C1–C6	124.7 (3)
C2–C1–C6	120.6 (3)	O1–C2–C1	115.3 (3)
O1–C2–C3	125.8 (3)	C1–C2–C3	118.9 (3)

C2–O1 length of the coordinated Phenox is 1.300 (4) Å, and the C1–N length is 1.363 (4) Å. Both values are 0.06 Å longer than values found for free PhenoxBQ and can be considered to be characteristic of the semiquinone form of the ligand, PhenoxSQ. The pattern of short and long C–C lengths within the quinone ring is retained. The C3–C4 and C5–C6 bonds are still the shortest of the ring lengths with values of 1.370 (6) and 1.372 (5) Å but are longer than the corresponding PhenoxBQ values.

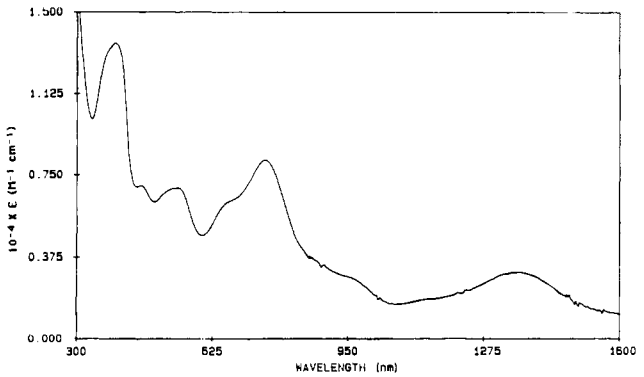

Figure 4. Electronic spectrum of $Ru(PPh_3)Cl(PhenoxSQ)_2$ recorded in dichloromethane solution.

Similar contraction in these ring C–C bond lengths is commonly found for coordinated semiquinone ligands.[12] Other features of the PhenoxSQ ligand are similar to those of PhenoxBQ, although, a fold of 9.6° at the O, N bridge between outer rings shows that it is less planar than the benzoquinone imine.

Structural features of $Ru(PPh_3)_2Cl_2(PhenoxSQ)$ indicate that the complex contains Ru(III) coordinated to the radical PhenoxSQ ligand. The diamagnetism must arise from strong antiferromagnetic coupling between the radical and the $S = {}^1/_2$ Ru(III) ion. The structure also provides metrical parameters for PhenoxSQ that may be useful in the determination of charge distribution from structural studies on other Phenox complexes.

Potentials obtained from electrochemical characterization on $Ru(PPh_3)_2Cl_2(PhenoxSQ)$ listed in Table VII consist of a reversible oxidation couple at 0.287 (86) V (vs Fc/Fc^+), with an additional irreversible oxidation at 0.584 V. The complex also undergoes reduction irreversibly at −1.119 V and this reduction is coupled with an oxidation at −0.604 V. Assignment of these processes is not unambiguous, but the reversible oxidation may be metal based as the Ru(III)/Ru(IV) couple. The related redox process for $Ru(PPh_3)_2Cl_2(DBSQ)$ appears at 0.297 V.[9] Other redox processes of the complex may occur at the Phenox ligand.

$Ru(PPh_3)Cl(PhenoxSQ)_2$. The reaction between $Ru(PPh_3)_3Cl_2$ and HPhenoxSQ carried out at a stoichiometry of 1:2 under an inert gas atmosphere has been found to produce $Ru(PPh_3)Cl(Phenox)_2$. The complex is a $S = {}^1/_2$ paramagnet and shows an electron paramagnetic resonance (EPR) spectrum at room temperature that consists of a single line centered at a g value of 1.996. The width of this line and the absence of hyperfine coupling are similar to spectra obtained on the $Ru(N–N)(DBSQ)_2^+$ complexes[13] but differ from the more complicated spectrum of the free PhenoxSQ radical.[10] The electronic spectrum of the complex, shown in Figure 4, consists of bands extending into the near-infrared region. Crystallographic characterization has shown that the Phenox ligands are coordinated at cis sites about the Ru as shown in Figure 5. Bond distances and angles for the complex are listed in Table IX. As with $Ru(PPh_3)_2Cl_2(PhenoxSQ)$, analysis of ligand bond lengths provides insight on charge distribution. Carbonyl bond lengths to the coordinated oxygen atoms are 1.314 (7) and 1.319 (7) Å for the C2–O1 and C30–O3 bonds. Lengths for the C–N bonds to the coordinated nitrogen atoms are 1.360 (7) and 1.368 (7) Å for the C1–N1 and C29–N2 bonds within the chelate ring. These values are shorter than the single C–N bonds to the carbon atoms of the outer aromatic ring which are 1.386 (7) Å for C7–N1 and 1.393 (7) Å for C35–N2. They are similar to the features of the PhenoxSQ ligand of $Ru(PPh_3)_2Cl_2(PhenoxSQ)$ and point to a semiquinone formulation for the Phenox ligands of $Ru(PPh_3)Cl(PhenoxSQ)_2$. Further confirmation for the semiquinone formulation for the Phenox ligands comes from the pattern of C–C bond lengths within the quinone ring. Values for the C–C bonds at positions that were localized double bonds for PhenoxBQ range from 1.373 (9) to 1.378 (9) Å. These are the shortest C–C lengths of the bonds in the ring but are longer than the corresponding lengths of PhenoxBQ. Both PhenoxSQ ligands are nonplanar with dihedral angles of 12.4° and 14.2° at the N–O bridges between the aromatic and quinone rings.

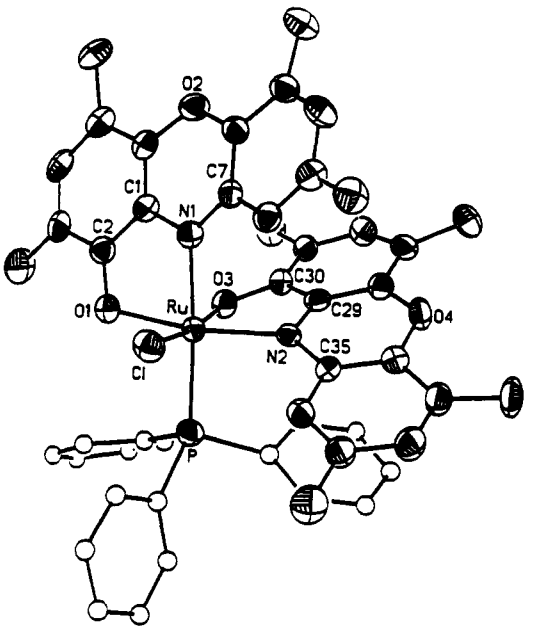

Figure 5. View of $Ru(PPh_3)Cl(PhenoxSQ)_2$.

Table IX. Selected Bond Lengths and Angles for $Ru(PPh_3)Cl(PhenoxSQ)_2$

	Lengths (Å)		
Ru–O1	2.034 (4)	Ru–O3	2.012 (4)
Ru–N1	2.052 (5)	Ru–N2	2.014 (4)
Ru–P	2.385 (2)	Ru–Cl	2.396 (2)
O1–C2	1.314 (7)	O2–C6	1.387 (7)
O2–C8	1.386 (7)	O3–C30	1.319 (7)
O4–C34	1.383 (7)	O3–C36	1.380 (7)
N1–C1	1.360 (7)	N1–C7	1.386 (7)
N2–C29	1.368 (7)	N2–C35	1.393 (7)
P–C57	1.825 (7)	P–C63	1.828 (6)
P–C69	1.840 (6)	C1–C2	1.432 (8)
C1–C6	1.403 (8)	C2–C3	1.408 (8)
C3–C4	1.378 (9)	C3–C13	1.507 (9)
C4–C5	1.409 (9)	C5–C6	1.373 (9)
C5–C17	1.551 (9)	C7–C8	1.397 (8)
C7–C12	1.400 (8)	C8–C9	1.400 (8)
C9–C10	1.388 (9)	C9–C21	1.537 (9)
C10–C11	1.393 (9)	C11–C12	1.385 (8)
C11–C25	1.526 (9)	C29–C30	1.421 (8)
C29–C34	1.407 (8)	C30–C31	1.403 (8)
C31–C32	1.378 (8)	C31–C41	1.529 (9)
C32–C33	1.410 (9)	C33–C34	1.377 (8)
C33–C45	1.527 (9)	C35–C36	1.398 (8)
C35–C40	1.394 (8)	C36–C37	1.408 (9)
C37–C38	1.390 (9)	C37–C49	1.542 (9)
C38–C39	1.385 (9)	C39–C40	1.380 (8)
C39–C53	1.543 (9)		
	Angles (deg)		
O1–Ru–O3	86.1 (2)	O1–Ru–N1	79.2 (2)
O3–Ru–N1	84.4 (2)	O1–Ru–N2	165.6 (2)
O3–Ru–N2	80.8 (2)	N1–Ru–N2	93.4 (2)
O1–Ru–P	93.9 (1)	O3–Ru–P	88.7 (1)
N1–Ru–P	170.5 (1)	N2–Ru–P	91.8 (1)
O1–Ru–Cl	90.7 (1)	O3–Ru–Cl	171.1 (1)
N1–Ru–Cl	86.9 (1)	N2–Ru–Cl	101.4 (1)
P–Ru–Cl	99.8 (1)	Ru–O1–C2	111.8 (3)
C6–O2–C8	118.6 (4)	Ru–O3–C30	110.3 (4)
C34–O4–C36	118.9 (4)	Ru–N1–C1	110.9 (4)
Ru–N1–C7	131.4 (4)	C1–N1–C7	117.2 (5)
Ru–N2–C29	109.6 (3)	Ru–N2–C35	133.9 (4)
C29–N2–C35	116.5 (4)		

(12) Boone, S. R.; Purser, G. H.; Chang, H.-R.; Lowery, M. D.; Hendrickson, D. N.; Pierpont, C. G. *J. Am. Chem. Soc.* **1989**, *111*, 2292.
(13) Haga, M.; Dodsworth, E. S.; Lever, A. B. P. *Inorg. Chem.* **1986**, *25*, 447.

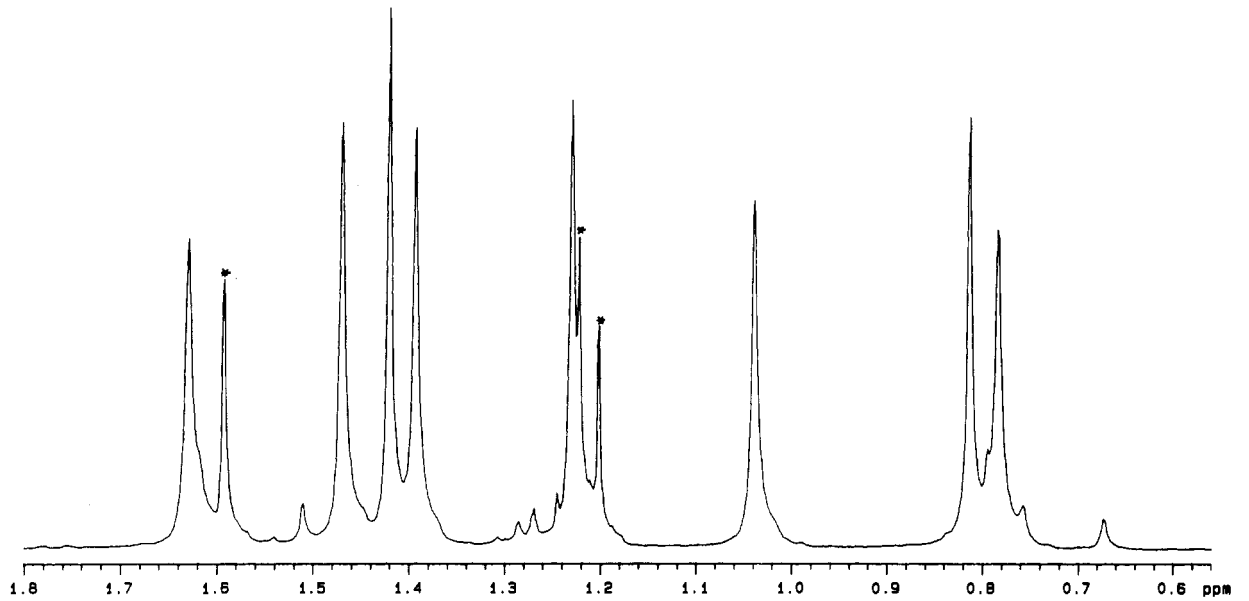

Figure 6. ^{1}H NMR spectrum in the *tert*-butyl methyl region recorded on a crude sample of $Ru(PPh_3)Cl(PhenoxSQ)(OxPhenox)$ isolated directly from the reaction mixture. Strong resonances of impurities are denoted with asterisks.

Structural features of the molecule point to a Ru(III) formulation for the complex as $Ru^{III}(PPh_3)Cl(PhenoxSQ)_2$. The $S = {}^1/_2$ magnetic ground state must result from strong coupling between the radical ligands and the paramagnetic metal, with residual spin density concentrated on the radical ligands. The absence of hyperfine in the EPR spectrum is not unusual for semiquinone complexes of Ru and may be due to delocalization between nominally equivalent PhenoxSQ ligands. The electrochemical properties of the complex shown in Figure 2 and listed in Table VII are pertinent to its chemical reactivity. It undergoes reversible reduction at −1.026 (94) V and shows two reversible oxidations at −0.254 (102) and 0.875 (92) V. Assignment of these couples is based on solution rest-potential measurements and on the electrochemical properties of other bis(PhenoxSQ) complexes containing metals which are not electroactive. The reduction appears to be metal based as the Ru(II)/Ru(III) couple, and the two oxidations occur at the PhenoxSQ ligands as PhenoxSQ/PhenoxBQ oxidations. Reduction of the complex would give the $Ru^{II}(PPh_3)Cl(PhenoxSQ)_2^-$ anion.

$Ru(PPh_3)Cl(PhenoxSQ)(OxPhenox)$. When carried out in air, the reaction between $Ru(PPh_3)_3Cl_2$ and HPhenoxSQ at a 1:2 stoichiometric ratio gives a product that is different than the $Ru(PPh_3)Cl(PhenoxSQ)_2$ product obtained under inert conditions. The product is diamagnetic and crude samples taken from the reaction mixture show eight *tert*-butyl resonances of equal intensity in the ^{1}H NMR spectrum. This spectrum is shown in Figure 6. Four of the resonances appear in the region between 1.1 and 1.5 ppm where PhenoxBQ and $Ru(PPh_3)_2Cl_2(PhenoxSQ)$ show *tert*-butyl resonances; the other four are on either side of this range. Crystallographic characterization on the complex shown in Figure 7, with metrical values listed in Table X, indicates that one of the Phenox ligands has been oxidized in the synthetic procedure. A view of the Ru(OxPhenox) region of the molecule is shown in Figure 8. Carbon atom C34, once contained in the quinone ring, is now associated with a carboxylate group that is coordinated to the Ru atom through oxygen O3. The other bond to the metal is through imine nitrogen N2 which is doubly bonded to carbon C29 with a N2–C29 length of 1.289 (18) Å. Three other carbon atoms that were formally associated with the quinone ring, C31, C32, and C33, are now contained in a dihydrofuran ring with a localized C–C double bond between C31 and C32. Three new oxygen atoms have been added to the PhenoxSQ ligand in the course of forming the OxPhenox ligand, the second carboxylate oxygen, the oxygen atom in the furan ring, and a hydroxyl group bound to carbon C33. Two chiral centers have been formed in this process, at carbon atoms C30 and C33, and oxygen atoms

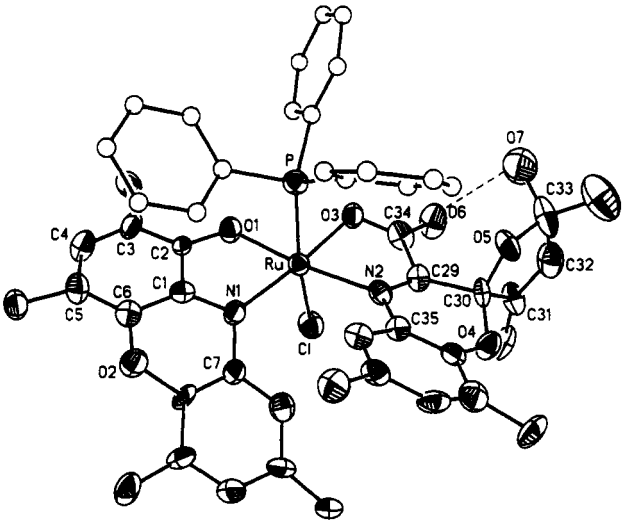

Figure 7. View of $Ru(PPh_3)Cl(PhenoxSQ)(OxPhenox)$.

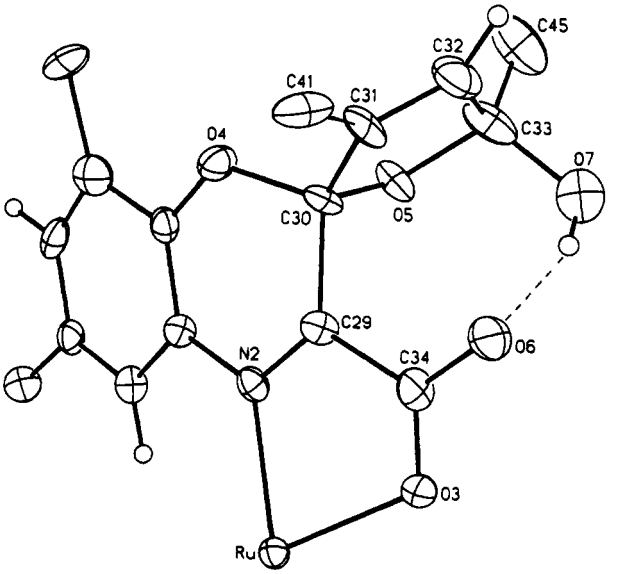

Figure 8. View of the Ru(OxPhenox) region of $Ru(PPh_3)Cl(PhenoxSQ)(OxPhenox)$.

O6 and O7 are separated by 2.81 Å indicating the presence of an intramolecular hydrogen bonding interaction with the hydroxyl

Table X. Selected Bond Lengths and Angles for $Ru(PPh_3)Cl(PhenoxSQ)(OxPhenox)$

Lengths (Å)			
Ru–Cl	2.406 (3)	Ru–P	2.381 (4)
Ru–O1	2.049 (7)	Ru–O3	2.032 (8)
Ru–N1	2.002 (12)	Ru–N2	2.143 (9)
P–C57	1.802 (11)	P–C63	1.347 (8)
P–C69	1.828 (7)	O1–C2	1.290 (16)
O2–C6	1.405 (11)	O2–C8	1.379 (15)
O3–C34	1.279 (18)	O4–C30	1.438 (14)
O4–C36	1.369 (16)	O5–C30	1.416 (16)
O5–C33	1.462 (25)	O6–C34	1.230 (19)
O7–C33	1.432 (19)	N1–C1	1.340 (17)
N1–C7	1.422 (14)	N2–C29	1.289 (18)
N2–C35	1.435 (12)	C1–C2	1.436 (14)
C1–C6	1.445 (19)	C2–C3	1.400 (17)
C3–C4	1.376 (20)	C3–C13	1.544 (15)
C4–C5	1.441 (15)	C5–C6	1.343 (18)
C5–C17	1.516 (23)	C7–C8	1.393 (22)
C7–C12	1.388 (19)	C8–C9	1.405 (16)
C9–C10	1.390 (20)	C9–C21	1.497 (24)
C10–C11	1.408 (23)	C11–C12	1.393 (17)
C11–C25	1.524 (20)	C29–C30	1.557 (20)
C29–C34	1.494 (15)	C30–C31	1.517 (21)
C31–C32	1.290 (24)	C31–C41	1.529 (21)
C32–C33	1.502 (23)	C33–C45	1.476 (32)
C35–C36	1.371 (17)	C35–C40	1.420 (19)
C36–C37	1.411 (15)	C37–C38	1.398 (22)
C37–C49	1.515 (20)	C38–C39	1.385 (21)
C39–C40	1.381 (15)	C39–C53	1.526 (22)
Angles (deg)			
Cl–Ru–P	166.4 (1)	Cl–Ru–O1	91.0 (3)
P–Ru–O1	85.9 (3)	Cl–Ru–O3	83.4 (3)
P–Ru–O3	83.6 (3)	O1–Ru–O3	94.3 (3)
Cl–Ru–N1	91.8 (3)	P–Ru–N1	100.4 (3)
O1–Ru–N1	77.4 (3)	O3–Ru–N1	170.4 (4)
Cl–Ru–N2	87.3 (3)	P–Ru–N2	93.7 (3)
O1–Ru–N2	170.9 (3)	O3–Ru–N2	76.6 (3)
N1–Ru–N2	111.6 (4)	Ru–P–C57	113.0 (3)
Ru–P–C63	118.8 (3)	C57–P–C63	103.4 (4)
Ru–P–C69	112.5 (3)	C57–P–C69	103.9 (4)
C53–P–C69	103.6 (4)	Ru–O1–C2	116.4 (6)
C6–O2–C8	118.7 (10)	Ru–O3–C34	115.2 (7)
C30–O4–C36	117.6 (9)	C30–O5–C33	109.0 (11)
Ru–N1–C1	115.2 (7)	Ru–N1–C7	130.2 (9)
C1–N1–C7	113.4 (11)	Ru–N2–C29	111.1 (7)
Ru–N2–C35	130.4 (8)	C29–N2–C35	118.4 (10)
N2–C29–C30	122.1 (10)	N2–C29–C34	116.1 (12)
C30–C29–C34	120.1 (12)	O4–C30–O5	110.1 (9)
O4–C30–C29	108.9 (12)	O5–C30–C29	105.9 (10)
O4–C30–C31	108.3 (10)	O5–C30–C31	105.9 (12)
C29–C30–C31	117.6 (10)	C30–C31–C32	107.8 (13)
C30–C31–C41	125.3 (14)	C32–C31–C41	126.8 (15)
C31–C32–C33	112.7 (17)	O5–C33–O7	109.4 (16)
O5–C33–C32	102.1 (14)	O7–C33–C32	112.8 (13)
O5–C33–C45	110.6 (14)	O7–C33–C45	105.2 (15)
C32–C33–C45	116.8 (18)	O3–C34–O6	125.8 (10)
O3–C34–C29	114.2 (12)	O6–C34–C29	119.7 (13)
N2–C35–C36	120.2 (11)	N2–C35–C40	119.4 (11)
C36–C35–C40	120.3 (10)		

proton.

The coordinated Phenox ligand has C–O and C–N lengths within the chelate ring of 1.290 (16) and 1.340 (17) Å, contracted ring bonds for C3–C4 and C5–C6, and a fold at the center nitrogen and oxygen atoms of 28.8°. These features are similar to the PhenoxSQ ligands of $Ru(PPh_3)_2Cl_2(PhenoxSQ)$ and $Ru(PPh_3)Cl(PhenoxSQ)_2$, and on this basis we assign the charge on the metal as Ru(III) with the diamagnetism of the complex arising from strong antiferromagnetic exchange between the paramagnetic metal and the radical ligand. The stereochemistry about the metal is also chiral, with phosphorus and chlorine atoms in trans coordination sites. Therefore, the centrosymmetric crystallographic unit cell consists of enantiomeric pairs of one diastereomer, and the NMR spectrum obtained on crude product from the reaction indicates that this is the only diastereomer formed in the synthetic procedure.

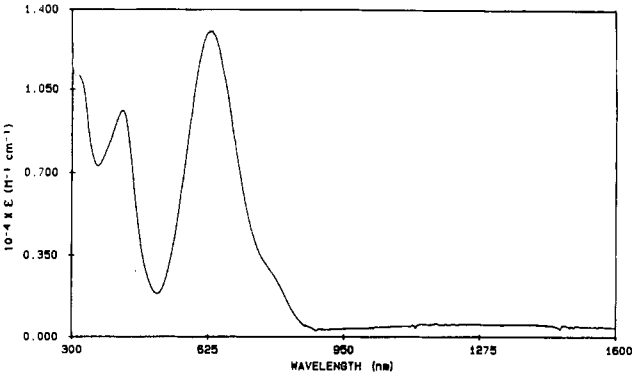

Figure 9. Electronic spectrum of $Ru(PPh_3)Cl(PhenoxSQ)(OxPhenox)$.

Electronic spectra on $Ru(PPh_3)Cl(PhenoxSQ)(OxPhenox)$ in the visible region (Figure 9) consist of bands at 422 nm (9800) and 632 nm (13100) with a low-energy shoulder at 779 nm. Electrochemical characterization on the complex consists of a reversible reduction at −0.933 (82) V and a reversible oxidation at +0.564(92) V (vs Fc/Fc^+). The reduction corresponds to the Ru(II)/Ru(III) couple and the oxidation to a ligand-based $PhenoxSQ^-/PhenoxBQ$ process.

Formation of $Ru(PPh_3)Cl(PhenoxSQ)(OxPhenox)$. The oxygen sensitivity of the reaction between HPhenoxSQ and $Ru(PPh_3)_3Cl_2$ is of interest. A common product that appears to form initially in both procedures is $Ru^{II}(PPh_3)Cl(PhenoxSQ)_2^-$. It probably forms as the cis isomer due to the steric interactions between *tert*-butyl substituents that would exist for chelated, coplanar Phenox ligands in a trans isomer. Electrochemical characterization on $Ru^{III}(PPh_3)Cl(PhenoxSQ)_2$ has shown that the Ru(II)/Ru(III) couple occurs at a very negative potential, −1.02 V, and the reduced Ru(II) form of the complex would be a strong reducing agent. Components in the reaction carried out under argon include PPh_3 and Cl^- displaced from $Ru(PPh_3)_3Cl_2$ and H^+ from HPhenoxSQ, in addition to $Ru^{II}(PPh_3)Cl(PhenoxSQ)_2^-$ formed initially in the reaction. The Ru(II) center of this complex would be quite able to reduce hydrogen ion in solution to give the Ru(III) product obtained experimentally. Hydrogen formed in this reaction has been difficult to detect experimentally due to the small quantity present, but there are no other components in the reaction that would be subject to reduction by the Ru(II) species. When carried out in air, oxygen is available as an oxidant for the Ru(II) complex, and the addition and reduction of molecular oxygen at the metal appears to occur as the initial step leading to intramolecular oxidation of one PhenoxSQ ligand to OxPhenox. Dissociation of the chloro ligand would provide a vacant site at the metal for oxygen coordination. There is literature precedent for this,[14] it is in accord with the change in stereochemistry at the metal, and the results of experimental attempts at reduction of $Ru(PPh_3)Cl(PhenoxSQ)_2$ are relevant. Coulometric reduction of the Ru(III) complex at a potential of −1.09 V using TBAP as the supporting electrolyte followed by exposure of the solution to air failed to produce $Ru(PPh_3)Cl(PhenoxSQ)(OxPhenox)$. However, synthetic reduction of $Ru(PPh_3)Cl(PhenoxSQ)_2$ using cobaltocene in dichloromethane followed by exposure of the solution to air led to formation of a product that gave the same optical spectrum as $Ru(PPh_3)Cl(PhenoxSQ)(OxPhenox)$. Failure of the coulommetry experiment may be related to the high concentration of electrolyte in solution with the perchlorate anion blocking the coordination site necessary for O_2 addition to the metal. The positive result obtained by chemical reduction of $Ru^{III}(PPh_3)Cl(PhenoxSQ)_2$ provides evidence that the Ru(II) form of the complex is the species oxidized by molecular oxygen in the formation of $Ru(PPh_3)Cl(PhenoxSQ)(OxPhenox)$.

Little direct evidence has been obtained for the mechanism of OxPhenox formation. Analytical difficulties in unambiguously

(14) Murray, K. S.; van den Bergen, A. M.; West, B. O. *Aust. J. Chem.* **1978**, *31*, 203.

Scheme I

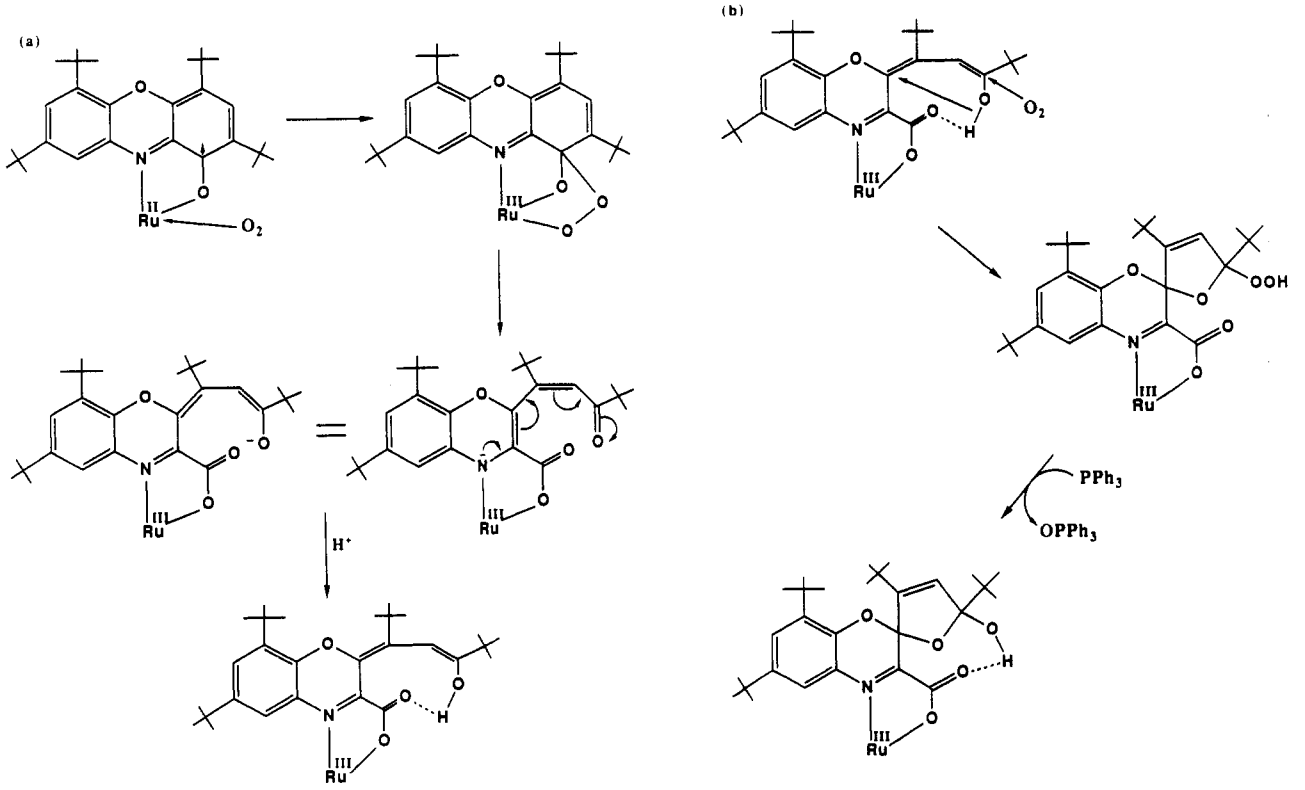

assigning label sites and label scrambling limit the utility of experiments carried out using isotopically labeled O_2. We have offered the mechanism shown in Scheme I to account for the oxidation, with knowledge of the stereochemical course of the reaction obtained from the X-ray structure and selectivity indicated by the ^1H NMR spectrum on crude product shown in Figure 6. Experiments carried out with the Ru(II) complex formed by reduction appear to indicate that initial attack by O_2 occurs at the nucleophilic metal. Addition of the resulting superoxide radical to the radical carbonyl carbon of one PhenoxSQ ligand would give the bridged peroxo species shown to form initially in the mechanism. A similar bridged peroxoquinone species has been proposed to form in the mechanism leading to catechol oxidation by the catechol dioxygenase enxymes,[3] and a complex containing a species of this form has recently been characterized structurally.[15] Rearrangement of the peroxoquinone intermediate to a dioxetane species (II) would ultimately lead to the ketocarboxylate through established mechanistic steps. It is of interest that this occurs at the C–C bond exo to the chelate ring to give a product similar to the species obtained from the extradiol dioxygenase enzymes,[16] rather than interior to the chelate ring to give an amidocarboxylate product. The reasons for this preference are not clear but may be stereochemical in origin.

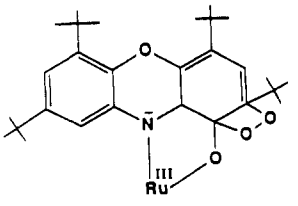

II

At this point in the mechanism the Phenox ring has been oxidatively cleaved, an electron has been added to the conjugated structure of the opened ring, and the metal has been oxidized to Ru(III). To obtain the OxPhenox product a second molecule of O_2 is needed. Selective attack of this oxygen molecule at a nucleophilic site on the opened ring defines the stereochemistry at both chiral carbon centers. It is likely that oxygen attack occurs selectively on the side of the molecular plane away from the triphenylphosphine ligand and this is consistent with the structure of the coordinated OxPhenox ligand. Protons present in solution from the protonated HPhenoxSQ starting material would add to the oxygen derived from the first oxidation step bonded to the carbon atom containing the *tert*-butyl group (III). Internal hydrogen bonding would retain the oxidized ring in a closed structure; rotation about C–C bonds to give an open structure would result in loss of stereochemical selectivity in the second oxidation step.

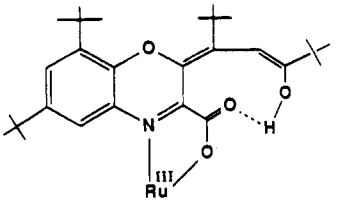

III

Oxidation by a second oxygen molecule which appears to add at the nucleophilic end carbon atom of the opened chain defines the stereochemistry at that center by formation of a hydroperoxide group. Hydroperoxides commonly react with triphenylphosphine to give triphenylphosphine oxide, and this reaction results in formation of the hydroxyl group at the end carbon. Also associated with this process is a cyclization step in which the dihydrofuran ring is formed and the stereochemistry at the second chiral site of OxPhenox is defined. Cyclization to form the C–O bond with O5 occurs at the side of the Phenox plane toward the coordinated triphenylphosphine ligand since rotation to allow attack from the opposite site would direct the *tert*-butyl group on carbon atom C33 into the phenyl rings of the ligand. Additionally, the assumption that oxygen attack on the opened ring occurs on the side away from the triphenylphosphine ligand requires that oxygen O5 in the product be derived from the alcohol rather than from the second oxygen molecule. Attack by the second oxygen

(15) Barbaro, P.; Bianchini, C.; Mealli, C.; Meli, A. *J. Am. Chem. Soc.* **1991**, *113*, 3181.
(16) (a) Arciero, D. M.; Lipscomb, J. D. *J. Biol. Chem.* **1986**, *261*, 2170. (b) Mabrouk, P. A.; Orville, A. M.; Lipscomb, J. D.; Solomon, E. I. *J. Am. Chem. Soc.* **1991**, *113*, 4053.

molecule and cyclization occur either in concert or in rapid sequence, for bond rotation within the conjugated ring-opened enol would result in loss of stereoselectivity and a mixture of diastereomeric products would result. Hydrogen bonding with the carboxylate oxygen is likely important in retaining the closed structure for the ring-opened conjugated alcohol chain.

Conclusions

The coordination chemistry of the Phenox quinone imine ligand differs from the complexes of ruthenium formed with the *o*-quinone and semiquinone ligands in the accessibility of the fully reduced amidophenolate or catecholate analogue. The reduction potential for the PhenoxSQ anion is considerably more negative than the Cat/SQ couple of the quinone ligands. Reduction of $Ru(PPh_3)Cl(PhenoxSQ)_2$ occurs at the metal to give a nucleophilic Ru(II) complex, while reduction of a corresponding $Ru^{III}(SQ)_2$ species occurs at the quinone ligands giving a much less reactive product. Oxidation reactions that utilize molecular oxygen are of commercial interest,[17] and they are pertinent to the stereoselective substrate oxidation reactions of enzymes.[18] The striking and surprising oxidation reaction leading to formation of the OxPhenox ligand may parallel the oxidation of coordinated catechol ligands. Generally, oxidative cleavage of the ring occurs at the C–C bond internal to the chelate ring in a manner that is typical of the intradiol dioxygenase enzymes. The reaction leading to the OxPhenox ligand proceeds by cleavage of the ring bond exterior to the chelate ring to give a product that might arise from a reaction that parallels the extradiol dioxygenase enzymes. Selectivity in this reaction appears to result from the effects of intramolecular hydrogen bonding with steric direction provided by the triphenylphosphine ligand and the Phenox *tert*-butyl groups. This combination of properties contributes to the formation of a single diasteromeric product with three chiral centers.

Acknowledgment. We gratefully acknowledge the help of Dr. Steven Boone with the crystallographic investigations. This research was supported by the National Science Foundation through Grants CHE-88-09923 and CHE-90-23636; ruthenium trichloride was provided by Johnson Matthey, Inc., through their Metal Loan Program.

Supplementary Material Available: Tables giving crystal data and details of the structure determination, anisotropic thermal parameters, hydrogen atom locations, and bond lengths and angles for PhenoxBQ, $Ru(PPh_3)_2Cl_2(PhenoxSQ)$, and $Ru(PPh_3)Cl(Phenox)_2$ (47 pages); listings of observed and calculated structure factors (49 pages). Ordering information is given on any current masthead page.

(17) Riley, D. P.; Fields, D. L.; Rivers, W. *J. Am. Chem. Soc.* **1991**, *113*, 3371.
(18) Smith, J. R. L.; Mortimer, D. N. *J. Chem. Soc., Chem. Commun.* **1985**, 64.

Contribution from the Departments of Chemistry, Southwest Texas State University, San Marcos, Texas 78666, Howard University, Washington, D.C., and Keene State College, Keene, New Hampshire 03431

Synthesis, Structure, and Spectroscopic Properties of Vanadium(III) and -(IV) Complexes Containing Hydridotris(pyrazolyl)borate Ligands. 3

Madan Mohan,[†] Stephen M. Holmes,[†] Ray J. Butcher,[‡] Jerry P. Jasinski,[§] and Carl J. Carrano*,[†]

Received September 26, 1991

A series of vanadium(III) and -(IV) complexes of the type $[L_2V]BPh_4$, $[LVCl_2DMF]$, [LVOClDMF], and [LVO(acac)] where L is either the anion of hydridotris(pyrazolyl)borate, $HB(pz)_3$, or hydridotris(3,5-dimethylpyrazolyl)borate, $HB(Me_2pz)_3$, have been synthesized and characterized by elemental analysis, molar conductance, electrochemistry, magnetic, UV–vis, IR, and ESR techniques. In all cases, the metal ion is in a distorted octahedral environment, facially coordinated to a tridentate hydridotris(pyrazolyl)borate ligand of varying steric bulk. The structures of the complexes of the type $[L_2V]BPh_4$ have been determined by single-crystal X-ray diffraction. Crystal data for $[[HB(pz)_3]_2V]BPh_4$ are as follows: space group $P\bar{1}$ with a = 12.796 (1) Å, b = 15.305 (2) Å, c = 11.285 (1) Å, α = 94.38 (1)°, β = 104.248 (9)°, γ = 108.64 (1)°, V = 2000.7 (5) Å^3, and Z = 2. In general, comparison of the structural and physicochemical properties among the series reveals the expected effects of the electron-releasing methyl groups but few if any differences between analogous complexes that can be attributed to steric bulk. However, electrochemistry does demonstrate significant differences between the unsubstituted and 3,5-dimethyl-substituted derivatives not evident from structural parameters which indicate a reduced access to the metal in the latter. The significance of these data to our understanding of vanadium centers in biological systems is discussed.

In a series of previous publications,[1-3] we and others have examined some of the chemistry of vanadium(III), -(IV), and -(V) with the hydridotris(3,5-dimethylpyrazolyl)borate ligand as a model for vanadium–histidine interactions that could be present in proteins such as the haloperoxidases from marine algae and terrestrial lichens.[4-7] Most of these complexes contain the hydridotris(3,5-dimethylpyrazolyl)borate group coordinated to the vanadium in a tridentate fashion leaving open another three coordination sites for ancillary ligands to complete a distorted octahedral environment around the metal ion. Since one of the unique ligating effects of a protein involves its ability to restrict access to a metal center, we were curious how such steric effects might be reflected in the structural and/or physicochemical properties of model complexes. Accordingly, we have synthesized and examined a series of analogous complexes using both the unsubstituted and the 3,5-dimethyl-substituted pyrazolylborate ligands. These ligands have respective "wedge angles" of 120° and 91° which reflect in a qualitative way the ease of access to the metal.[8] In this paper, we report that while structural differences between the substituted and unsubstituted complexes are insignificant, electrochemistry clearly reveals an increased accessibility to the metal center in the latter. It is anticipated that these results may aid in our understanding of the nature of va-

[†] Southwest Texas State University.
[‡] Howard University.
[§] Keene State College.

(1) Kime-Hunt, E.; Spartalian, K.; DeRusha, M.; Nunn, C. M.; Carrano, C. J. *Inorg. Chem.* **1989**, *28*, 4392.
(2) Holmes, S. M.; Carrano, C. J. *Inorg. Chem.* **1991**, *30*, 1231.
(3) Collison, D.; Mabbs, F. E.; Passand, M. A.; Rigby, K.; Cleland, W. E. *Polyhedron* **1989**, *8*, 1827.
(4) Vilter, H. *Phytochemistry* **1984**, *23*, 1387.
(5) Plat, H.; Krenn, B. E.; Wever, R. *Biochem. J.* **1987**, *248*, 277.
(6) van Kooyk, Y.; de Boer, E.; Tromp, M. G. M.; Plat, H.; Wever, R. *Biochim. Biophys. Acta* **1986**, *869*, 48.
(7) Butler, A.; Carrano, C. J. *Coord. Chem. Rev.* **1991**, *109*, 61.
(8) Calabrese, J. C.; Domaille, P. J.; Trofimenko, S.; Long, G. J. *Inorg. Chem.* **1991**, *30*, 2795.

0020-1669/92/1331-2029$03.00/0